



## Article

# Study on Performance Comparison of Two Hydrogen Liquefaction Processes Based on the Claude Cycle and the Brayton Refrigeration Cycle

Jian Yang <sup>1</sup>, Yanzhong Li <sup>1,2</sup>  and Hongbo Tan <sup>1,\*</sup> <sup>1</sup> Department of Refrigeration and Cryogenic Engineering, Xi'an Jiaotong University, Xi'an 710049, China<sup>2</sup> State Key Laboratory of Technologies in Space Cryogenic Propellants, Beijing 100028, China

\* Correspondence: hongbotan@xjtu.edu.cn

**Abstract:** Hydrogen liquefaction is an essential section for efficient storage and transportation of hydrogen energy. Both the Claude cycle and Brayton refrigeration cycle are available for large-scale hydrogen liquefaction systems. Two large-scale hydrogen liquefiers with the liquefaction capacity of 120 t/d based on the Brayton refrigeration cycle and the Claude cycle, respectively, are analyzed and compared in this study. Sensitivity analysis is used to optimize the parameters of two liquefaction systems in HYSYS. According to the results, the exergy loss and specific energy consumption of the Claude liquefier are 18.98 MW and 5.62 kWh/kg<sub>LH</sub>, which are 6.6% and 4.4% less than those of the Brayton liquefier, respectively. Exergy analysis reveals the exergy loss of compression and expansion systems in the Claude liquefier is less than that of the Brayton liquefier, while the exergy loss of the throttle valve in the Claude liquefier is more notable. In addition, the molar flow rate of hydrogen used as refrigerant in the Claude liquefier is 10.6% less than that of refrigerant in the Brayton liquefier. Owing to the smaller size requirements of equipment and the lower specific energy consumption, the Claude cycle is more suitable for large-scale hydrogen liquefaction processes.

**Keywords:** Claude cycle; Brayton refrigeration cycle; performance comparison; exergy analysis



**Citation:** Yang, J.; Li, Y.; Tan, H. Study on Performance Comparison of Two Hydrogen Liquefaction Processes Based on the Claude Cycle and the Brayton Refrigeration Cycle. *Processes* **2023**, *11*, 932. <https://doi.org/10.3390/pr11030932>

Academic Editor: Adam Smoliński

Received: 17 February 2023

Revised: 13 March 2023

Accepted: 16 March 2023

Published: 18 March 2023



**Copyright:** © 2023 by the authors. Licensee MDPI, Basel, Switzerland. This article is an open access article distributed under the terms and conditions of the Creative Commons Attribution (CC BY) license (<https://creativecommons.org/licenses/by/4.0/>).

## 1. Introduction

Fossil energy sources, including oil and coal, have dominated the world's energy system from the last century to the present [1]. In the last 100 years, serious environmental and ecological problems have emerged all over the world. In order to get out of the dilemma, in recent years, the development trend of global energy system is transforming towards decarbonization [2]. As a clean energy source, hydrogen is considered the ideal new generation of energy with zero pollution and high calorific value [3]. It is not only the best choice for deep and large-scale decarbonization in the future energy sector, but the best carrier for the conversion and storage of renewable energy to avoid imbalance between supply and demand [4]. Nevertheless, the development of hydrogen energy still faces bottlenecks in terms of efficient transportation and storage [5]. The methods include compression, physical adsorption, liquefaction, metal hydrides and complex hydrides that can be adopted to storage hydrogen [6]. Among them, hydrogen storage technologies such as liquid hydrogen (LH), methylcyclohexane and ammonia are attracting high attention [4]. The application of LH is more promising, considering the high purity requirements for its future utilization (e.g., fuel cells) and the development of transoceanic trade [7].

Hydrogen liquefaction cycles mainly consist of the Linde-Hampson (L-H) cycle and the Claude cycle [8]. In the L-H cycle, the hydrogen is expanded in the Joule-Thompson (J-T) throttle, while in the Claude cycle, this step is achieved in the expander. The Claude cycle exhibits higher liquefaction rate and lower energy consumption than the L-H cycle, but requires more investment costs [9]. As a result, the L-H cycle is suitable for small-scale hydrogen liquefaction plants, while the Claude cycle is considered for large-scale hydrogen

liquefaction plants [10]. In addition, the hydrogen can be liquefied using a closed external refrigeration cycle, which is typified by the Brayton refrigeration cycle. Like the L-H cycle, the Brayton refrigeration cycle used to be considered appropriate for small-scale hydrogen liquefaction processes. However, it has been applied frequently in the recent literature studying large-scale hydrogen liquefaction systems [10]. Therefore, the Claude cycle is compared with the Brayton refrigeration cycle in various aspects to assess the feasibility of application to large-scale hydrogen liquefaction plants.

The classic Claude cycle consists of a refrigeration loop with an expander in which the liquefied hydrogen is depressurized through the J-T throttle and then becomes the qualified product. Cammarata et al. [11] improved the classic Claude cycle that can be used for the liquefaction of helium or hydrogen. The refrigeration loop in the improved Claude cycle contained two expanders in series, and a heat exchanger was incorporated between them. Tarique et al. [12] replaced the J-T throttle in a classic Claude cycle with an expander and found that this not only reduced the energy consumption of the cycle, but recovered work. Nevertheless, more consideration was needed in the selection of the expander because the expansion process involved two-phase flow. Baker et al. [13] conducted a parametric study for a hydrogen liquefier equipped with a dual-pressure Claude cycle. The exergy efficiency and specific energy consumption (SEC) of this liquefier were calculated to be 36% and 10.5 kWh/kg<sub>LH</sub>, respectively.

Recently-constructed hydrogen liquefaction plants around the world were based on improved Claude cycles. Among them, the representative Linde hydrogen liquefier in Germany has improved the refrigeration loop in the Claude cycle by using three expanders in series [10]. The SEC of the liquefier was 11.9 kWh/kg<sub>LH</sub>, which was more efficient than the plant at Ingolstadt [14]. In addition, the hydrogen liquefaction plants in Praxair, USA, implemented an improved two-stage Claude cycle. In these plants, the pressure drop of the refrigerant in the different refrigeration loops was different, which facilitated the performance. An amount of 12.5–15 kWh/kg<sub>LH</sub> were considered the typical SEC values for Praxair plants, and the exergy efficiency was between 19.3% and 24% [10]. In a conceptual hydrogen liquefier based on a three-stage Claude cycle proposed by Kuendig et al. [15], the three-stage refrigeration loops were arranged in a crossover pattern instead of the conventional series mode. Liquid nitrogen and LNG were used for the hydrogen pre-cooling in this liquefier with a SEC of 4.0 kWh/kg<sub>LH</sub>. In addition, a hydrogen liquefier based on a two-stage Claude cycle with the cross-arranged refrigeration loops was proposed by Cardella et al. [16]. This improved Claude cycle with the assistance of mixed refrigerant pre-cooling had exergy efficiency and SEC of 43% and 6.2 kWh/kg<sub>LH</sub>, respectively, and was considered one of the most promising hydrogen liquefier design options. In the hydrogen liquefaction system integrated with biomass gasification proposed by Ebrahimi et al. [17], the Claude cycle was employed to liquefy hydrogen with a coefficient of performance of up to 4.360. In addition, the Claude cycle has also been employed in several hydrogen liquefaction process concepts that combined renewable energy sources such as geothermal and solar energy [18–20].

Numerous hydrogen liquefaction process concepts were developed based on the Brayton refrigeration cycles. Li et al. [21] incorporated a Brayton refrigeration cycle to an L-H cycle-based hydrogen liquefaction process, which significantly increased the liquefaction rate of the system. In addition, they developed a generic model to analyze the effects of multiple parameters in the system. Quack et al. [22] developed a helium-neon Brayton refrigeration cycle with a self-cooling heat exchanger in a hydrogen liquefier. The SEC of this liquefier was reported to be 5.0 kWh/kg<sub>LH</sub>, and the exergy efficiency can reach 60%. A large-scale hydrogen liquefaction process using four Brayton cycles was proposed by Krasae-in et al. [23], and they analyzed the effects of the pinch temperature and pressure drop in the heat exchanger on the simulation results. They found the SEC of the system increased from 5.0 kWh/kg<sub>LH</sub> at a pinch temperature of 1 °C to 5.20 kWh/kg<sub>LH</sub> at a pinch temperature of 3 °C. Connecting multiple refrigeration loops in series in a single refrigeration cycle is more compact than connecting multiple Brayton refrigeration cycles in

direct series. Valenti et al. [24] investigated the performance of a novel Brayton cycle with four refrigeration loops for hydrogen liquefaction. An exergy efficiency of approximately 48% can be achieved in this novel Brayton refrigeration cycle, known as the four-stage Joule-Brayton (J-B) cycle. Park et al. [25] proposed two different J-B cycles including a dual-pressure cycle and a split triple-pressure cycle. Owing to the division of the pressure levels of the different refrigeration loops in the triple-pressure cycle, it was more energy efficient and cost effective. The SEC of the liquefier using the triple-pressure cycle was 5.69 kWh/kg<sub>LH</sub>, which was 3.2% lower than that of the base process.

The Claude cycle is widely used in existing hydrogen liquefaction plants, while the Brayton refrigeration cycle is the most popular in recent hydrogen liquefaction concept designs. Both cycles are considered suitable for large-scale hydrogen liquefaction processes, however, no studies have been conducted to quantitatively compare their performance in hydrogen liquefaction. Therefore, the presented work aims to provide a comparative analysis of these two cycles. Both hydrogen liquefiers using two different cycles are modeling in HYSYS and the process parameters are determined by performing sensitivity analysis. The performance parameters, including exergy efficiency and SEC of two liquefiers, are compared and analyzed in terms of heat exchange efficiency and exergy loss. Eventually, the prospects of two different hydrogen liquefaction processes applied to large-scale hydrogen liquefaction systems are assessed.

## 2. Process Description and Modeling

### 2.1. Description of the Processes

Two hydrogen liquefaction processes compared in this study employ a two-stage Claude cycle and a two-stage J-B refrigeration cycle, respectively. Each refrigeration loop in the two processes is composed of two expanders connected in series.

In the Claude liquefaction process (Claude liquefier) as illustrated in Figure 1, the feed hydrogen is first mixed with the refluxed hydrogen that has been pressurized by compression systems, and then provided with pre-cooling by liquid nitrogen. The pre-cooled hydrogen is split twice at different temperatures, and the hydrogen that is split out acts as the refrigerant in the refrigeration loops to provide cooling for the remaining hydrogen. The cooled hydrogen passes through the conversion reactor to increase the proportion of para-hydrogen and reduces the pressure through the J-T valve before entering the gas-liquid separator. The cryogenic hydrogen exiting the gas-liquid separator returns to the inlet of the liquefier after releasing its cold energy. The LH discharged from the liquid outlet of the gas-liquid separator is stored.

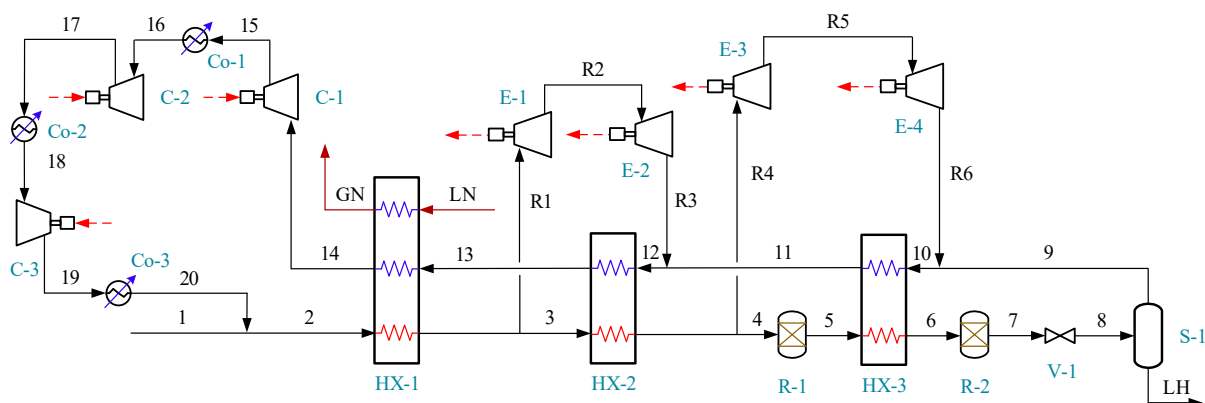


**Figure 1.** Schematic diagram of the Claude liquefier.

In the Brayton liquefaction process (Brayton liquefier) as illustrated in Figure 2, the hydrogen is pre-cooled by the liquid nitrogen with an equal flow rate as in the Claude liquefier. Thereafter, the Brayton refrigeration cycle provides the cold energy used for further cooling and liquefaction of hydrogen. In the Brayton refrigeration cycle, helium as

refrigerant is compressed by the three-stage compression system with interstage cooling. The compressed helium is divided into two streams and pre-cooled to different temperatures in the HX-4 and HX-5, respectively. They can provide cooling for hydrogen after expansion in each refrigeration loop. After passing through the conversion reactor to increase the proportion of para-hydrogen and the J-T valve to reduce the pressure in turn, the liquefied hydrogen is stored.

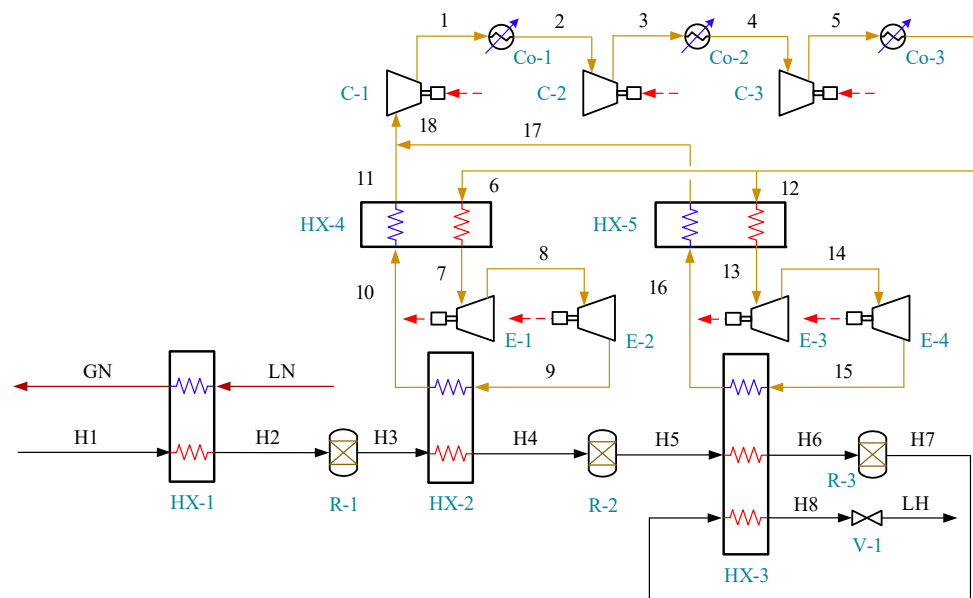


Figure 2. Schematic diagram of the Brayton liquefier.

2.2. Process Known Conditions

Two liquefiers are modeled in HYSYS which can realize fast and accurate calculation to provide a guarantee for the analysis and comparison of various process schemes. The Peng-Robinson equation, which is more accurate in thermal property calculations at low temperatures than the SRK, and BWRS equation [26], is selected as the equation of state for the process simulation. To make the comparison results more convincing, the pre-cooling temperature of hydrogen, the isentropic efficiency of expanders and compressors, the pinch temperature of heat exchangers, the cooling temperature provided by coolers, and the proportion of para-hydrogen in the LH are all the same in both liquefiers. Known parameters applicable to the two liquefiers are listed in Table 1.

Table 1. The known parameters in two hydrogen liquefiers.

Feed parameter	
Mass flow rate (t/d)	120
Para-hydrogen proportion (%)	25
Pressure (kPa)	2100
Temperature (°C)	25
Product parameter	
Para-hydrogen proportion (%)	>95
Pressure (kPa)	130
Temperature (°C)	−252.5

**Table 1.** *Cont.*

Equipment parameter	
Compressors (isentropic efficiency, %)	80
Coolers (cooling temperature, °C)	25
Expanders (isentropic efficiency, %)	85
Heat exchangers (minimum temperature approach, °C)	1
Liquid nitrogen parameter	
Temperature (°C)	−196
Pressure (kPa)	101
Mass flow rate (t/h)	40

### 2.3. Conversion between Para- and Ortho-Hydrogen

The hydrogen molecule is made up of two atoms. Bonhoeffer et al. [27] found that the two nuclei in the hydrogen molecule exhibited different spin directions, and they had different optical and thermodynamic properties. Therefore, the hydrogen is divided into two types. Hydrogen molecules made up of two atoms with parallel spin directions are named ortho-hydrogen, while those made up of two atoms with antiparallel spin directions are named para-hydrogen. The hydrogen is an equilibrium mixture, and the equilibrium state is principally determined by the temperature [28]. At the room temperature, the proportion of ortho-hydrogen is approximately 75%. When the temperature changes, the two types of hydrogen will interconvert and eventually reach equilibrium. However, the conversion is extremely slow and is accompanied by the release of a considerable amount of heat, which is sufficient to cause the vaporization of LH. Therefore, catalysts need to be considered to accelerate the conversion in the liquefaction process. The conversion between ortho- and para-hydrogen is carried out under adiabatic condition in this study, and the detailed simulation method is available in a previous study [29].

### 2.4. Thermodynamic Analysis Models

Energy balance equations are the basis of the simulation calculation of liquefaction process, and the exergy equation is essential for the thermodynamic analysis of each equipment. For the chemical equipment involved in the process, the applicable thermodynamic equations are listed in Table 2. Moreover, the exergy efficiency of the equipment is necessary to be considered in the thermodynamic analysis. Input-output efficiency and consumed-produced efficiency are the two forms used to characterize the exergy utilization efficiency in the equipment [30]. Among them, the latter better reflects the real operation of the equipment. Therefore, the consumed-produced efficiency of the relevant equipment can be calculated using the formula in Equation (1).

$$\varepsilon = \frac{\text{Useful Exergy Output}}{\text{Useful Exergy Input}} \quad (1)$$

where  $\varepsilon$  is the exergy efficiency of equipment.

**Table 2.** Exergy and energy equations of the key equipment.

Equipment	Energy Equation	Exergy Equation
Heat exchanger	$\sum \dot{m}_h \cdot (h_{in} - h_{out})_h = \sum \dot{m}_c \cdot (h_{out} - h_{in})_c$	$\dot{I}_{HX} = \sum \dot{m}_{HX} \cdot (e_{in} - e_{out})$
Compressor	$\dot{W}_C = \dot{m}_C \cdot (h_{out} - h_{in})$	$\dot{I}_C = \dot{W}_C - \dot{m}_C \cdot [e_{out} - e_{in}]$
Expander	$\dot{W}_E = \dot{m}_E \cdot (h_{in} - h_{out})$	$\dot{I}_E = \dot{m}_E \cdot (e_{in} - e_{out}) - \dot{W}_E$
Valve	$h_{V, in} = h_{V, out}$	$\dot{I}_V = \dot{m}_V \cdot (e_{in} - e_{out})$
Cooler	$\dot{Q}_{Co} = \dot{m}_{Co} \cdot (h_{out} - h_{in})$	$\dot{I}_{Co} = \dot{m}_{Co} \cdot (e_{in} - e_{out})$

The energy required for the liquefier comes from the energy consumption in compression systems, and the work recovered by expanders is assumed to drive compressors entirely. Therefore, the energy used to produce each kilogram of LH (SEC) can be expressed as Equation (2).

$$\text{SEC} = \frac{\dot{W}_{\text{net}}}{\dot{m}_{\text{LH}}} = \frac{\sum \dot{W}_{\text{C-i}} - \sum \dot{W}_{\text{E-i}}}{\dot{m}_{\text{LH}}} \quad (2)$$

where  $\dot{W}_{\text{net}}$  is net power required for liquefying hydrogen;  $\dot{W}_{\text{E}}$  is output work rate of expanders;  $\dot{W}_{\text{C}}$  is consumed work rate of compressors;  $\dot{m}_{\text{LH}}$  is mass flow rate of LH.

In addition to energy, the liquefier can be assessed from the perspective of exergy. Hydrogen liquefaction process is a process of exergy increasing, and the source of exergy is the energy input. Therefore, the ratio of the increase in the exergy of hydrogen to the net energy required in the hydrogen liquefier can be expressed as the exergy efficiency [31], as shown in Equation (3).

$$\eta = \frac{\dot{W}_{\text{min}}}{\dot{W}_{\text{net}}} = \frac{\dot{m}_{\text{LH}}(e_{\text{LH}} - e_{\text{Feed}})}{\dot{W}_{\text{net}}} \quad (3)$$

where  $e_{\text{Feed}}$  and  $e_{\text{LH}}$  are the mass exergy of feed hydrogen and LH, respectively.

### 3. Results and Analysis

#### 3.1. Sensitivity Analysis

In this study, sensitivity analysis is employed to optimize stream parameters for both liquefiers. The cooling temperature of hydrogen ( $t_{\text{R4}}$ ) is the only parameter affecting the performance of the Claude liquefier, because the feed parameters, the product parameters and the pre-cooling temperature of hydrogen are constant values. The effect of  $t_{\text{R4}}$  on the SEC of the Claude liquefier is given in Figure 3. The SEC of the Claude liquefier shows a trend of monotonically decreasing with the increase in  $t_{\text{R4}}$ . During the increase in  $t_{\text{R4}}$  from  $-229$  °C to  $-226$  °C, the SEC of the Claude liquefier is reduced from 6.88 to 5.62 kWh/kg<sub>LH</sub>, a reduction of up to 18.3%. Therefore, the selection of  $t_{\text{R4}}$  has a considerable influence on the SEC of the Claude liquefier. The system has requirements for the temperature that the refrigerant can reach in the second stage refrigeration loop. Therefore, the value of  $t_{\text{R4}}$  only can be increased to  $-226$  °C, as shown in Figure 3.

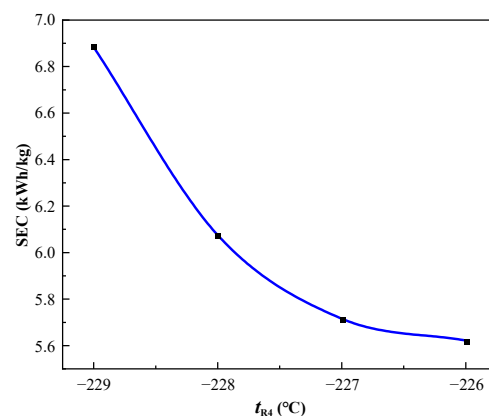


**Figure 3.** Effect of  $t_{\text{R4}}$  on the SEC of the Claude liquefier.

In the Brayton liquefier, the pressurization pressure of helium ( $p_5$ ) and the cooling temperature of hydrogen ( $t_{\text{H4}}$ ) are key parameters affecting the process performance. Among them, the effect of  $t_{\text{H4}}$  on the Brayton liquefier is similar to that of  $t_{\text{R4}}$  on the Claude liquefier. Therefore, only the effects of  $p_5$  on the Brayton liquefier are analyzed, as shown in Figure 4. As the pressure increases, the mass flow rate of the refrigerant required for the Brayton liquefier keeps decreasing, while the SEC of the Brayton liquefier is first decreasing and then increasing. There is a value of helium pressurization pressure that minimizes the

SEC of the Brayton liquefier. The helium pressurization pressure should be determined by considering various aspects such as equipment safety, operation costs, and investment costs. In this study, this pressure value is determined as 1400 kPa, owing to the minimum SEC.

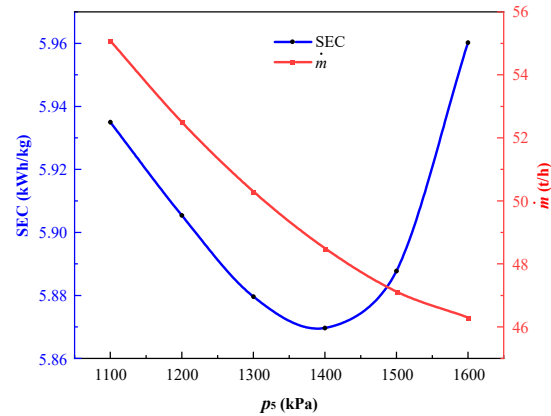


**Figure 4.** Effects of  $p_5$  on the Brayton liquefier.

### 3.2. Performance Comparison between Processes

The comparison of the performance parameters including SEC, molar flow rate of refrigerant, and exergy loss between the two liquefiers is shown in Figure 5. The SEC of the two liquefiers is 5.62 kWh/kg<sub>LH</sub> and 5.87 kWh/kg<sub>LH</sub>, respectively. The SEC of the Claude liquefier is 4.4% less than that of the Brayton liquefier. In addition, the exergy efficiencies of the Claude and the Brayton liquefiers are 54.2% and 53.2%, respectively. Higher efficiency and lower energy consumption have made the Claude cycle a popular choice for the hydrogen liquefaction plants that have been built.

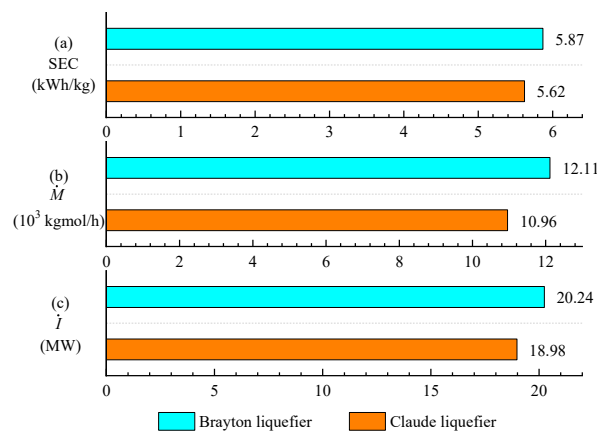


**Figure 5.** Performance parameters of two liquefiers: (a) SEC, (b) molar flow rate of refrigerant, and (c) exergy loss.

The molar flow rates of hydrogen as refrigerant in the Claude liquefier and helium in the Brayton liquefier are compared, as shown in Figure 5b. The molar flow rate of refrigerant in the Claude liquefier is 10.6% less than that of refrigerant in the Brayton liquefier, which implies that the volume flow rate of associated equipment in the Brayton liquefier is greater than that of equipment in the Claude liquefier. In particular, the pressurization pressure of hydrogen in the Claude liquefier is considerably higher than that of helium in the Brayton liquefier, which results in more than twice the volume flow rate of the high-pressure refrigerant in heat exchangers in the Brayton liquefier than that of the refrigerant in the Claude liquefier. Therefore, the scale of equipment including heat exchangers, expanders and compressors in the Claude liquefier is smaller than those in the Brayton liquefier, thus reducing investment costs. In addition, the exergy loss of both liquefiers is given in

Figure 5c. The exergy loss of the Claude liquefier is 18.98 MW, which is 6.6% less than the 20.24 MW of the Brayton liquefier. A detailed analysis of the exergy loss will be given in Section 3.4.

### 3.3. Composite Curve Analysis

Composite curves of the heat exchangers including HX-1 and HX-3 in two liquefiers are analyzed. Figure 6a,b give the composite curves of HX-1 used for hydrogen pre-cooling in each liquefier, respectively. The hydrogen in two liquefiers is pre-cooled using liquid nitrogen with the same mass flow rate. Because liquid nitrogen releases a considerable amount of cold energy at a constant temperature during the gasification process, a great heat exchange temperature difference is generated in HX-1. Unlike the Brayton liquefier, the cryogenic hydrogen from the gas-liquid separator serves as the cold stream in HX-1 in the Claude liquefier. The maximum heat exchange temperature difference in HX-1 in the Brayton liquefier exceeds 100 °C, while this parameter is only approximately 20 °C in the Claude liquefier. The results indicate that the liquid nitrogen is utilized more efficiently in the Claude liquefier owing to the presence of two cold streams. Therefore, integrating the helium self-precooling process in HX-4 and HX-5 with the liquid nitrogen pre-cooling process can enhance the performance of the Brayton liquefier through increasing the utilization efficiency of liquid nitrogen. However, because the energy demand of the pre-cooling process only accounts for approximately 20% of total energy [25], the effect achieved by the above improvement is limited.

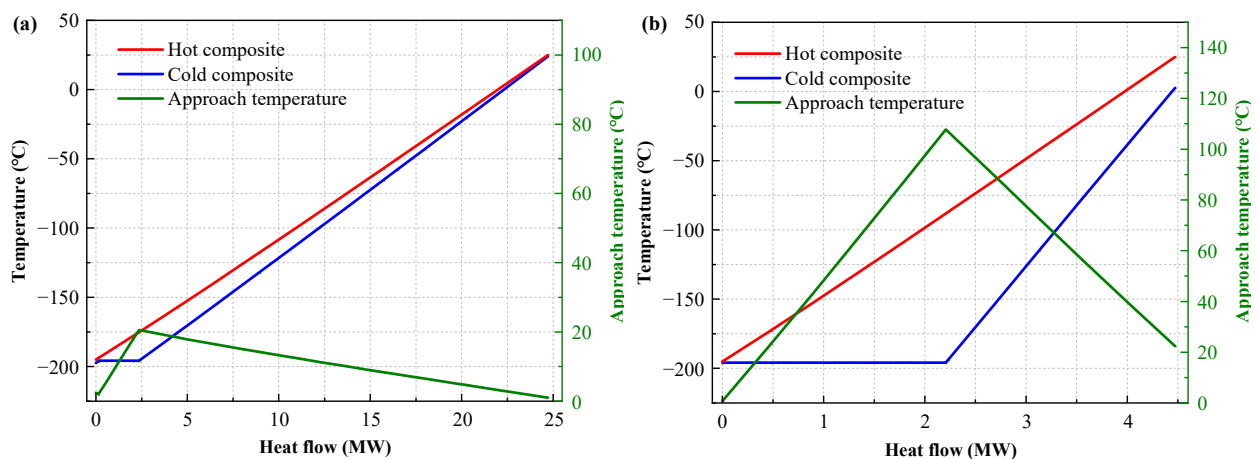


**Figure 6.** Composite curves of HX-1 in each liquefier: (a) Claude liquefier, and (b) Brayton liquefier.

Figure 7a,b give the composite curves of HX-3 used to liquefy and sub-cool the hydrogen in the two liquefiers, respectively. Overall, the composite curves shown in both figures are similar. Slightly different is that the LH in the Brayton liquefier needs to be further sub-cooled because the temperature of LH rises after the conversion in R-3, which increases the minimum temperature approach in HX-3. In addition, the mass flow rate of hydrogen being cooled in the Claude liquefier is greater than that of hydrogen in the Brayton liquefier because it cannot be completely liquefied, which results in a considerable difference in the heat flow rate between the two heat exchangers. As far as the heat exchange process is concerned, the advantage of the Claude liquefier over the Brayton liquefier is the superior cold energy utilization of liquid nitrogen, while its disadvantage is the heavy heat exchange load at cryogenic temperatures.

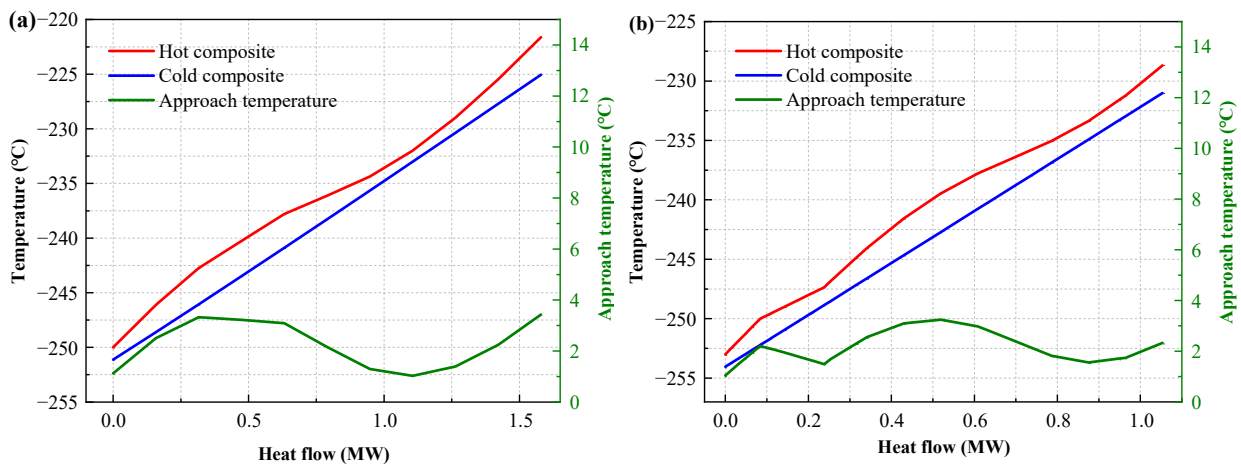


Figure 7. Composite curves of HX-3 in each liquefier: (a) Claude liquefier, and (b) Brayton liquefier.

### 3.4. Exergy Analysis

Exergy analysis, including exergy efficiency and exergy loss, is performed for the equipment in both liquefiers. Figure 8 gives the comparison of the exergy loss between different types of equipment in the two liquefiers, and Figure 9 gives the comparison of the exergy efficiency between the corresponding equipment in the two liquefiers. The pressure ratios of compressors in the Claude liquefier are higher than those in the Brayton liquefier, so they exhibit more exergy loss and lower exergy efficiency. However, in the Brayton liquefier, a significant amount of exergy in the streams from the compressor outlet is lost in the coolers, which is 31.2% higher than that in the Claude liquefier. Therefore, the exergy loss of compression systems containing compressors and coolers in the Claude liquefier is smaller than that of compression systems in the Brayton liquefier. The expansion ratios of expanders in the Claude liquefier are smaller than those of expanders in the Brayton liquefier, yet they exhibit less exergy loss and higher exergy efficiency. It can be inferred that the refrigeration effect of hydrogen in the Claude liquefier is considerably better than that of helium in the Brayton liquefier.

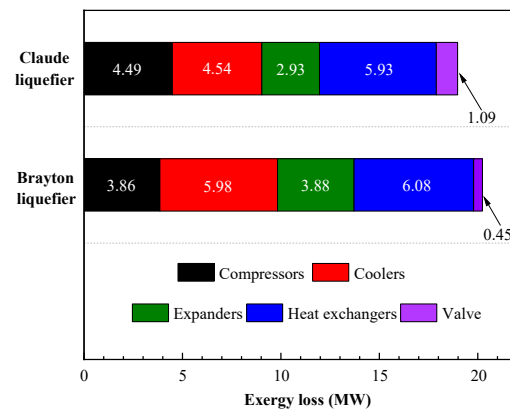
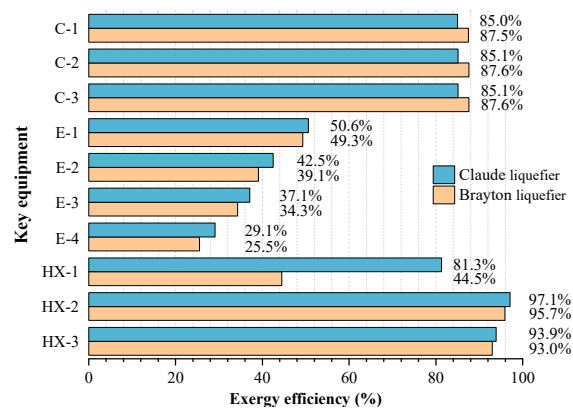


Figure 8. The comparison of the exergy loss for different types of equipment in the two liquefiers.

Due to the gasification of liquid nitrogen, the exergy efficiencies of HX-1 in both liquefiers are inefficient, especially in the Brayton liquefier. The exergy efficiencies of other heat exchangers in both liquefiers are excellent, with either heat exchanger exceeding 93%. In contrast to the poor compressibility, both hydrogen and helium have a better heat transfer capability [32]. The J-T valve is the key equipment in the hydrogen liquefier. As showed in Figure 8, the exergy loss of J-T valve in the Claude liquefier is more than twice that of J-T valve in the Brayton liquefier. On the one hand, because the Claude cycle is a non-complete liquefaction cycle, the mass flow rate of LH through J-T valve in the Claude

liquefier is considerably more than that in the Brayton liquefier. On the other hand, in the Claude liquefier, liquid hydrogen appears in two-phase flow during the throttling process, which further increases the exergy loss in the J-T valve. Overall, owing to the higher exergy efficiency of compression and expansion systems, exergy loss of the Claude liquefier is 6.6% lower than that of the Brayton liquefier.



**Figure 9.** The comparison of exergy efficiency between the corresponding equipment.

#### 4. Conclusions

In this study, two hydrogen liquefaction processes (the Claude liquefier and the Brayton liquefier) with the liquefaction capacity of 120 t/d are compared and analyzed. The simulation models of two hydrogen liquefiers are developed in HYSYS, and the parameters of both liquefiers are determined through sensitivity analysis. Further, performance parameters including SEC, molar flow rate of refrigerant, and exergy loss are compared between the two liquefiers. Finally, the compression, expansion, heat exchange, and throttling systems in both liquefiers are compared by composite curve analysis and exergy analysis.

According to the results, the SEC of the Claude liquefier is 5.62 kWh/kg<sub>LH</sub>, which is 4.4% less than 5.87 kWh/kg<sub>LH</sub> of the Brayton liquefier, which implies that the Claude liquefier has lower operating costs. In addition, the molar flow rate of hydrogen used as refrigerant in the Claude liquefier is 3.04 kgmol/s, which is 10.6% less than that of helium in the Brayton liquefier, which indicates a smaller size requirement for the associated equipment in the Claude liquefier. Exergy analysis reveals the exergy loss of compression and expansion systems in the Claude liquefier is less than that of the Brayton liquefier, while the exergy loss of J-T valve in the Claude liquefier is more notable. Overall, the exergy loss of the Claude liquefier is 18.98 MW, which is 6.6% less than that of the Brayton liquefier.

Owing to the smaller size requirements of the equipment and the lower energy consumption, the Claude cycle is more suitable for large-scale hydrogen liquefaction plants. It is evidenced by the preference of existing hydrogen liquefaction plants for the Claude cycle. However, the Brayton refrigeration-cycle-based hydrogen liquefaction process is easier to modularize in terms of operation and management, so it has the potential to be applied in the future. Improvements of the Claude liquefier should be aimed at increasing the hydrogen liquefaction rate. In addition, replacing the J-T valve with a liquid phase expander may enhance the performance of the Claude liquefier significantly. For the Brayton liquefier, it is imperative to develop the mixed refrigerant with better compressibility and refrigeration properties to improve the performance of the compression and expansion processes.

**Author Contributions:** J.Y.: Investigation, Conceptualization, Methodology, Software, Writing—original draft. Y.L.: Investigation, Methodology, Writing—review and editing, H.T.: Investigation, Methodology, Funding acquisition, Supervision. All authors have read and agreed to the published version of the manuscript.

**Funding:** This research was funded by the National Natural Science Foundation of China (Grants No: 51876153) and National Key Research and Development Program (No: 2020YFB1506203).

**Data Availability Statement:** Not applicable.

**Conflicts of Interest:** The authors declare that they have no known competing financial interests or personal relationships that could have appeared to influence the work reported in this paper.

## References

1. Sun, H.; Geng, J.L.; Wang, C.; Rong, G.X.; Gao, X.Y.; Xu, J.M.; Yang, D.C. Optimization of a hydrogen liquefaction process utilizing mixed refrigeration considering stages of ortho-para hydrogen conversion. *Int. J. Hydrogen Energy* **2022**, *47*, 17271–17284. [[CrossRef](#)]
2. Wijayanta, A.T.; Oda, T.; Purnomo, C.W.; Kashiwagi, T.; Aziz, M. Liquid hydrogen, methylcyclohexane, and ammonia as potential hydrogen storage: Comparison review. *Int. J. Hydrogen Energy* **2019**, *44*, 15026–15044. [[CrossRef](#)]
3. Jackson, S.; Brodal, E. Optimization of a mixed refrigerant based H<sub>2</sub> liquefaction pre-cooling process and estimate of liquefaction performance with varying ambient temperature. *Energies* **2021**, *14*, 6090. [[CrossRef](#)]
4. Andersson, J.; Gronkvist, S. Large-scale storage of hydrogen. *Int. J. Hydrogen Energy* **2019**, *44*, 11901–11919. [[CrossRef](#)]
5. Lee, S.-Y.; Lee, J.-H.; Kim, Y.-H.; Kim, J.-W.; Lee, K.-J.; Park, S.-J. Recent progress using solid-state materials for hydrogen storage: A short review. *Processes* **2022**, *10*, 304. [[CrossRef](#)]
6. Zhou, L. Progress and problems in hydrogen storage methods. *Renew. Sust. Energy Rev.* **2005**, *9*, 395–408. [[CrossRef](#)]
7. Zhao, Y.X.; Gong, M.Q.; Yuan, Z.; Dong, X.Q.; Jun, S. Thermodynamics analysis of hydrogen storage based on compressed gaseous hydrogen, liquid hydrogen and cryo-compressed hydrogen. *Int. J. Hydrogen Energy* **2019**, *44*, 16833–16840.
8. Hookham, M.J.F.; Le Gendre, E.; Couplier, C.; Carré, M.; Morris, A.S.O.; Moore, N.; Hristova, Y.; Bacquart, T. Impact of hydrogen liquefaction on hydrogen fuel quality for transport applications (ISO-14687:2019). *Processes* **2022**, *10*, 1697. [[CrossRef](#)]
9. Nandi, T.K.; Sarangi, S. Performance and optimization of hydrogen liquefaction cycles. *Int. J. Hydrogen Energy* **1993**, *18*, 131–139. [[CrossRef](#)]
10. Al Ghafri, S.; Munro, S.; Cardella, U.; Funke, T.; Notardonato, W.; Trusler, J.M.; Leachman, J.; Span, R.; Kamiya, S.; Pearce, S. Hydrogen liquefaction: A review of the fundamental physics, engineering practice and future opportunities. *Energy Environ. Sci.* **2022**, *15*, 2690. [[CrossRef](#)]
11. Cammarata, G.; Fichera, A.; Guglielmino, D. Optimization of a liquefaction plant using genetic algorithms. *Appl. Energy* **2001**, *68*, 19–29. [[CrossRef](#)]
12. Tarique, A.; Dincer, I.; Zamfirescu, C. Application of scroll expander in cryogenic process of hydrogen liquefaction. In *Progress in Exergy, Energy, and the Environment*; Springer: Cham, Switzerland, 2014; pp. 91–97.
13. Baker, C.R.; Shaner, R.L. A study of the efficiency of hydrogen liquefaction. *Int. J. Hydrogen Energy* **1978**, *3*, 321–334. [[CrossRef](#)]
14. Bracha, M.; Lorenz, G.; Patzelt, A.; Manner, M. Large-scale hydrogen liquefaction in Germany. *Int. J. Hydrogen Energy* **1994**, *19*, 53–59. [[CrossRef](#)]
15. Kuendig, A.; Loehlein, K.; Kramer, G.J.; Huijsmans, J. Large scale hydrogen liquefaction in combination with LNG re-gasification. In Proceedings of the 16th World Hydrogen Energy Conference, Lyon, France, 13–16 June 2006; pp. 3326–3333.
16. Cardella, U.; Decker, L.; Klein, H. Roadmap to economically viable hydrogen liquefaction. *Int. J. Hydrogen Energy* **2017**, *42*, 13329–13338. [[CrossRef](#)]
17. Ebrahimi, A.; Ghorbani, B.; Ziabasharhagh, M. Pinch and sensitivity analyses of hydrogen liquefaction process in a hybridized system of biomass gasification plant, and cryogenic air separation cycle. *J. Clean. Prod.* **2020**, *258*, 120548. [[CrossRef](#)]
18. Kaşka, Ö.; Yılmaz, C.; Bor, O.; Tokgoz, N. The performance assessment of a combined organic Rankine-vapor compression refrigeration cycle aided hydrogen liquefaction. *Int. J. Hydrogen Energy* **2018**, *43*, 20192–20202. [[CrossRef](#)]
19. Meng, Y.; Wu, H.Y.; Zheng, Y.H.; Wang, K.P.; Duan, Y.Y. Comparative analysis and multi-objective optimization of hydrogen liquefaction process using either organic Rankine or absorption power cycles driven by dual-source biomass fuel and geothermal energy. *Energy* **2022**, *253*, 124078. [[CrossRef](#)]
20. Mehrenjani, J.R.; Gharehghani, A.; Sangesarakki, A.G. Machine learning optimization of a novel geothermal driven system with LNG heat sink for hydrogen production and liquefaction. *Energy Convers. Manag.* **2022**, *254*, 115266. [[CrossRef](#)]
21. Li, K.Y.; Zhang, S.G.; Liu, G.L. Model for analyzing the energy efficiency of hydrogen liquefaction process considering the variation of hydrogen liquefaction ratio and precooling temperature. *Int. J. Hydrogen Energy* **2022**, *47*, 24194–24211. [[CrossRef](#)]
22. Quack, H. Conceptual design of a high efficiency large capacity hydrogen liquefier. *AIP Conf. Proc.* **2002**, *613*, 255–263.
23. Krasae-In, S. Optimal operation of a large-scale liquid hydrogen plant utilizing mixed fluid refrigeration system. *Int. J. Hydrogen Energy* **2014**, *39*, 7015–7029. [[CrossRef](#)]

24. Valenti, G.; Macchi, E. Proposal of an innovative, high-efficiency, large-scale hydrogen liquefier. *Int. J. Hydrogen Energy* **2008**, *33*, 3116–3121. [[CrossRef](#)]
25. Park, S.; Noh, W.; Park, J.; Park, J.; Lee, I. Efficient heat exchange configuration for sub-cooling cycle of hydrogen liquefaction process. *Energies* **2022**, *15*, 4560. [[CrossRef](#)]
26. Azizabadi, H.R.; Ziabasharhagh, M.; Mafi, M. Applicability of the common equations of state for modeling hydrogen liquefaction processes in Aspen HYSYS. *Gas Process. J.* **2021**, *9*, 11–28.
27. Bonhoeffer, K.; Harteck, P. Experimente über para-und orthowasserstoff. *Naturwissenschaften* **1929**, *17*, 182. [[CrossRef](#)]
28. Harkness, R.W.; Deming, W.E. The equilibrium of para and ortho Hydrogen. *J. Am. Chem. Soc.* **1932**, *54*, 2850–2852. [[CrossRef](#)]
29. Yang, J.; Li, Y.Z.; Tan, H.B.; Bian, J.; Cao, X.W. Optimization and analysis of a hydrogen liquefaction process integrated with the liquefied natural gas gasification and organic Rankine cycle. *J. Energy Storage* **2023**, *59*, 106490. [[CrossRef](#)]
30. Cao, X.W.; Yang, J.; Zhang, Y.; Gao, S.; Bian, J. Process optimization, exergy and economic analysis of boil-off gas reliquefaction processes for LNG carriers. *Energy* **2022**, *242*, 122947. [[CrossRef](#)]
31. Bian, J.; Yang, J.; Li, Y.X.; Chan, Z.Q.; Liang, F.C.; Cao, X.W. Thermodynamic and economic analysis of a novel hydrogen liquefaction process with LNG precooling and dual-pressure Brayton cycle. *Energy Convers. Manag.* **2021**, *250*, 114904. [[CrossRef](#)]
32. Sadaghiani, M.S.; Mehrpooya, M. Introducing and energy analysis of a novel cryogenic hydrogen liquefaction process configuration. *Int. J. Hydrogen Energy* **2017**, *42*, 6033–6050. [[CrossRef](#)]

**Disclaimer/Publisher’s Note:** The statements, opinions and data contained in all publications are solely those of the individual author(s) and contributor(s) and not of MDPI and/or the editor(s). MDPI and/or the editor(s) disclaim responsibility for any injury to people or property resulting from any ideas, methods, instructions or products referred to in the content.